

# Boundary Condition Identification Based on 3D Photoelasticity

M. L. L. Wijerathne\*, Kenji Oguni\*\* and Muneo Hori\*\*\*

\*M.Eng., Graduate student, Dept. of Civil Eng., Univ. of Tokyo, (1-1-1, Yayoi, Bunkyo, Tokyo, 113-0032)

\*\*Ph.D., Research Assoc., Earthquake Research Ins., Univ. of Tokyo, (1-1-1, Yayoi, Bunkyo, Tokyo, 113-0032)

\*\*\*Ph.D., Professor, Earthquake Research Ins., Univ. of Tokyo, (1-1-1, Yayoi, Bunkyo, Tokyo, 113-0032)

A new numerical algorithm for nondestructive identification of the boundary conditions applied on a 3D body based on photoelasticity is developed. This new method for boundary conditions identification is based on the load incremental approach, which linearizes the nonlinear governing equation of photoelasticity by considering small increments of applied load. In an earlier attempt, a method for stress identification in a 3D body was developed based on load incremental approach by the authors. In this new attempt, the earlier method is strengthened by applying the equilibrium constraint and instead of directly identifying the state of stress, identification of boundary conditions is considered. The use of equilibrium constraint not only reduces the computational cost but also stabilizes the numerical scheme in the load incremental approach

**Key Words :** 3D photoelasticity, boundary conditions identification, load incremental approach, nonlinear inverse analysis

## 1. Introduction

Unstable crack growth under compression in 3D bulk bodies is an important phenomena in engineering. Since the failure mechanisms are governed by the state of stress, a nondestructive and full field measurement system for 3D state of stress is needed. The currently available 3D stress measurement techniques have limitations in their applications due to their destructive property, limitations in identifiable state of stress, etc.. Because of these limitations in currently available systems, development of a nondestructive and full field 3D stress measurement system is a prior requirement for investigating the mechanism for failure under compression. In this paper, an attempt to develop such a measurement technique is explained.

First, the nature of 3D photoelasticity should be explained. Propagation of polarized light ray in the direction of  $z$  axis through an elastically deformed photoelastic medium under an arbitrary 3D state of stress is governed by the following equation<sup>1)</sup> named as the *optical equation of photoelasticity*.

$$\frac{d\mathbf{A}}{dz} = \mathbf{GA}, \quad (1)$$

where  $\mathbf{A}$  represents the light vector,  $(A_x, A_y)^T$ , propagating in  $z$  direction and transformation matrix,

$$\mathbf{G} = -\frac{1}{2}iC_0 \begin{bmatrix} \sigma_{xx} - \sigma_{yy} & 2\sigma_{xy} \\ 2\sigma_{xy} & \sigma_{yy} - \sigma_{xx} \end{bmatrix}$$

$A_x$  and  $A_y$  ( $\in C$ ) denote the components of light vector along the axes  $x$  and  $y$  of an orthogonal coordinate system  $x, y$  and  $z$ ;  $C_0$  is a material constant for a given medium;  $\sigma_{xx}, \sigma_{yy}$  and  $\sigma_{xy}$  ( $\in \Re$ ) are the stress components in  $xy$  plane; and  $i$  is the unit of imaginary number.

According to the Eq. (1), output light carries information of state of stress on planes perpendicular to the light propagation direction in an integrated form. The inverse problem of photoelasticity is to identify the state of stress in a body based on the measurements on output light from many different directions (Fig. 1). This is a nonlinear inverse problem which is regarded as a tensor filed tomographic problem.

Conventional methods of 3D photoelasticity avoid this nonlinearity either based on 2D concept (e.g. scattered light photoelasticity and frozen stress photoelasticity) or assumption of weak birefringence (e.g. integrated photoelasticity). These have limitations in applications due to their destructive property, limitations in identifiable state of stress, etc..

In an earlier attempt<sup>2)</sup>, a load incremental approach for identification of 3D state of stress based

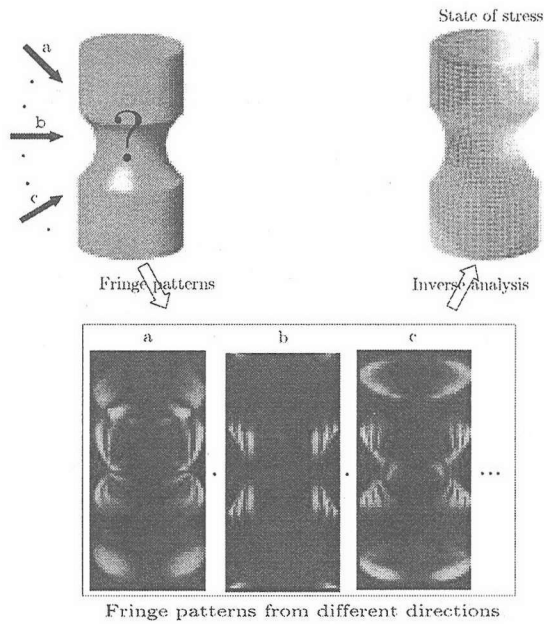


**Fig. 1** The inverse problem of photoelasticity is to identify the state of stress based on the transmitted light patterns from many different directions

on photoelasticity was developed by the authors. This was an attempt to solve the inverse problem of photoelasticity by linearizing the nonlinear governing equation of photoelasticity, considering the change in state of stress due to small load increments. As long as the load increments are small, this method can be successfully employed to identify the history of state of stress in a 3D body.

For linear elastic materials, when boundary conditions are given, everything can be completely determined based on the equilibrium equations. Consider the goal of this research, identification of stress distribution around a 3D crack under compression. In this case, if the boundary conditions on the surface of the linear elastic body and the traction on crack surface can be identified, the stress or strain distribution in the whole body is completely determined. In fact, the problem of identifying the state of stress (large number of unknowns) is reduced to a problem of identifying traction/displacement boundary conditions (less number of unknowns).

In this paper, incremental method for identification of boundary conditions (traction/displacement) applied on a linear elastic body is presented. This method can be regarded as an introduction of equilibrium constraint to the former load incremental ap-

proach for 3D photoelasticity. The use of equilibrium constraint not only drastically reduces the computational cost by reducing the number of unknowns, but also stabilizes the numerical scheme in the presence of measurement error in input data set for inverse analysis.

Details of the load incremental approach for stress identification without equilibrium constraint is given in the second section while the details of incremental approach for boundary conditions identification is presented in the third section. In the fourth section, a numerical example for validation of the new method and some features important for experiment are presented.

## 2. Load incremental approach for stress identification

Before explaining the load incremental approach for stress identification, the difficulty in the inverse problem of photoelasticity should be explained.

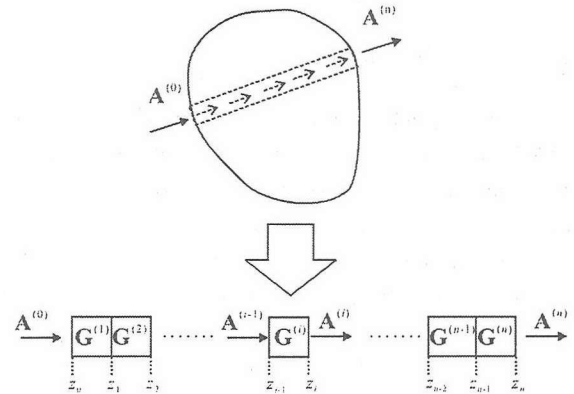


**Fig. 2** A light ray passing through a discretized object

Consider a light ray passing through an object (Fig. 2). The state of stress along the light ray is modelled with  $n$  number of elements each with constant state of stress. The light vectors  $A^{(i-1)}$  and  $A^{(i)}$  are input and output lights of the  $i^{th}$  element, and  $G^{(i)}$  is the transformation matrix of the  $i^{th}$  element. Based on the Eq. (1), an expression for output light  $A^{(n)}$  can be written in terms of input light  $A^{(0)}$  and transformation matrices  $G^{(i)}$  in each element.

$$A^{(n)} = (I + H^{(n)})(I + H^{(n-1)}) \dots (I + H^{(1)})A^{(0)} \quad (2)$$

where,  $\mathbf{I}$  is a  $2 \times 2$  identity matrix and  $\mathbf{H}^{(i)} = \mathbf{G}^{(i)}(z_i - z_{i-1})$ .

The output is expressed as a non-commutable multiplicative form of the matrices which are functions of unknown stress components. This is the source for nonlinear relation between the output light and the state of stress. The inverse problem of photoelasticity is fairly complicated as a result of this nonlinear relation.

The key to solve this nonlinear inverse problem is the linearization of the governing equation of photoelasticity considering the change in physical quantities due to a small load increment. Both the old method for stress identification and the new method for boundary conditions identification are based on this load incremental approach.

Consider the rate of change in the physical quantities in Eq. (2) with respect to small load increment,  $\Delta F$ .

$$\begin{aligned} \frac{\Delta \mathbf{A}^{(n)}}{\Delta F} = & \left[ \frac{\Delta \mathbf{H}^{(n)}}{\Delta F} (\mathbf{I} + \mathbf{H}^{(n-1)}) \dots (\mathbf{I} + \mathbf{H}^{(1)}) \right. \\ & + (\mathbf{I} + \mathbf{H}^{(n)}) \frac{\Delta \mathbf{H}^{(n-1)}}{\Delta F} \dots (\mathbf{I} + \mathbf{H}^{(1)}) \\ & + \vdots \\ & \left. + (\mathbf{I} + \mathbf{H}^{(n)}) (\mathbf{I} + \mathbf{H}^{(n-1)}) \dots \frac{\Delta \mathbf{H}^{(1)}}{\Delta F} \right] \mathbf{A}^{(0)} \end{aligned} \quad (3)$$

In Eq. (3), derivatives  $\Delta \mathbf{H}^{(i)}/\Delta F$  are linear functions of the stress increments in the  $i^{th}$  element,  $\Delta \sigma^{(i)}$ . With the knowledge of the current transformation matrices,  $\mathbf{H}^{(i)}$ , a function of the current state of stress ( $\sigma^{(i)}$ ), the increment of the output light vector,  $\Delta \mathbf{A}^{(n)}/\Delta F$ , can be expressed as a linear combination of the stress increment in each element,  $\Delta \sigma^{(i)}$ . Therefore, with enough number of experimental observations for  $\Delta \mathbf{A}^{(n)}/\Delta F$  for different light rays and the knowledge of the current  $\mathbf{H}^{(i)}$ , a set of independent linear equations for  $\Delta \sigma^{(i)}/\Delta F$  can be formed. This linearization process is the essence of the load incremental approach. Arranging the equations for different observation directions in the matrix form, a set of linearized equations can be obtained.

$$\Delta \mathbf{a} = \mathbf{M}(\sigma) \Delta \sigma \quad (4)$$

where,  $\mathbf{M}(\sigma)$  and  $\Delta \mathbf{a}$  are the assembly of right and left hand side of Eq. (3) for different observation directions.

This set of equations can be solved by the following standard iterative algorithm.

- (i) Initial values:  $\sigma^{[0]} = \sigma$ ,  $\Delta \sigma^{[0]} = 0$ , (where  $\sigma$  is the state of stress before the increment);
  - (ii)  $\begin{cases} \sigma^{[k+1]} = \sigma^{[k]} + \Delta \sigma^{[k]}, \\ \Delta \mathbf{a} = \mathbf{M}(\sigma^{[k]}) \Delta \sigma^{[k+1]} \end{cases}$  solve for  $\Delta \sigma^{[k+1]}$  where  $k$  is an iteration counter.
- Continue (ii) until  $\Delta \sigma^{[k+1]} \rightarrow 0$ ;
- (iii)  $\sigma = \sigma^{[k]}$ , (state of stress after the increment is obtained).

As long as the stress increments are small and no error in  $\mathbf{A}$ , this method can be successfully employed to identify the history of state of stress starting from stress free state<sup>2)</sup>. Unlike other approaches to 3D photoelasticity, make use of the history of the output light patterns to identify the history of state of stress is the most distinct feature of this method.

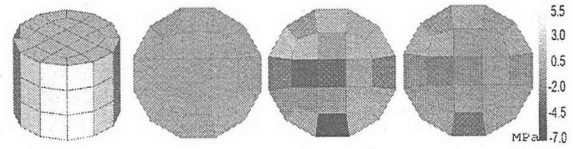


Fig. 3 Discretized cylindrical object and the vertical stress components assigned to each layer

% error in measurements	% error in predictions
0.1	21.3
0.5	106.7
1	233.3

Table 1 Error in predictions due to measurement errors

As a numerical test to judge the effect of presence of noise in output light measurements, a cylindrical object was modelled with 63 elements and assigned a set of random numbers to represent the state of stress (Fig. 3). The output light were calculated from many different directions. Then the state of stress was changed by adding or subtracting a random number to the original values and output light were calculated for the same observation directions. A random error (adding or subtracting a random value between 0 and a given percentage of maximum input light intensity) was introduced to all the calculated output light intensities, and inverse analysis was performed to identify the effect of presence of noise. Results of this analysis is given in Table 1. According to these

results, small error in output light measurements magnifies the error in predictions.

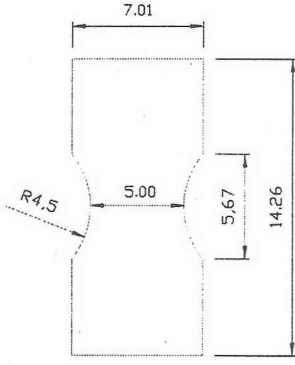


Fig. 4 Dimensions of the grooved cylinder used for simulations. Units in *mm*.

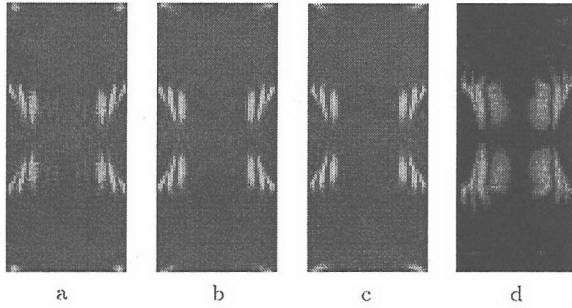


Fig. 5 Comparison of fringe patterns for different discretizations with the experimental results. a) 5632 elements, b)  $8 \times 5632$  elements, c)  $64 \times 5632$  elements and d) Experimental results

As a preliminary test to judge the necessary number of discretization for the load incremental approach for stress identification, a grooved cylinder (Fig. 4) under uniform compression in axial direction was modelled with different number of elements and the fringe pattern from each model was numerically calculated. Fig. 5 shows the numerical results for different discretizations and the experimental result. According to these results, a few hundred thousands elements are necessary for qualitative reproduction of experimental images. Therefore, when this stress inverse method is used, large number of degrees of freedom is involved.

In the next section, an attempt to introduce the equilibrium constraint to the load incremental approach and thereby reducing the number of unknowns and increasing the robustness of this method against

the presence of noise in measurements is explained.

### 3. Load incremental approach for identification of boundary conditions

In this section a new method for identification of history of boundary conditions on a linear elastic body by introducing the equilibrium constraint to the load incremental approach is explained. Based on this new technique, the traction distribution on a crack surface in a 3D body under compression can be identified. Since the state of stress/strain in a linear elastic body can be completely determined by the known boundary conditions and the equilibrium constraint, the state of stress around the crack can be determined. Thereby the goal of this research is achieved.

In this method complicated boundary conditions applied on a 3D body is modelled as a linear combination of finite number of independent set of traction/displacement distributions (modes) and the stress distribution in the body due to each of these modes is found by finite element method or boundary element method. A better approximation for applied boundary conditions can be achieved by including higher modes. The aim of the inverse analysis of boundary conditions is to identify the increments of amplitudes of each traction/displacement mode due to small load increment.

The transformation matrix  $\mathbf{H}^{(i)}$  can be expressed as a linear combination of transformation matrices due to each traction mode.

$$\mathbf{H}^{(i)} = \mathbf{g}_k^{(i)} f_k (z_i - z_{i-1}) \quad k = 1 \dots N \quad (5)$$

where  $\mathbf{g}_k^{(i)}$  is the transformation matrix in  $i^{th}$  element due to the  $k^{th}$  mode and  $f_k$  is the amplitude of  $k^{th}$  mode. Note that unbracketed repeating indices denote the summation.

Substitution of this expression in Eq. (2) shows that the output light and unknown amplitudes for traction modes are related by a multiplicative form. Therefore, the relation between the output light and amplitudes of traction modes is nonlinear.

When the instantaneous state of stress due to each mode and their amplitudes are known, substitution of Eq. (5) in Eq. (3) gives a linear relation between the output light increment  $\Delta \mathbf{A}^{(n)}$  and increments of mode amplitudes,  $\Delta f_k$  for the next increment. Once,

enough number of observations from different directions are made for output light increments,  $\Delta A^{(n)}$ , and if  $g_k^{(i)}$  and current  $f_k$  are known, an independent set of linear equations can be obtained for increments of mode amplitudes,  $\Delta f_k$ . This set of equations can be solved for increments of mode amplitudes by the same standard iterative updating algorithm used in stress inversion discussed in the previous section. Then the state of stress is found by superposition of each state of stress due to traction modes.

A major advantage of this new method is the reduction of large number of unknown stress terms involved in stress inversion to less number of boundary conditions. The exact number of unknowns involved in boundary condition identification depends on the complexity of the boundary condition applied on the body. In addition to that, the stress state obtained from traction inversion method always satisfies the equilibrium constraint since it is obtained as a linear combination of state of stress due to each mode considered in the inverse analysis.

## 4. Numerical results

### 4.1 Example problem

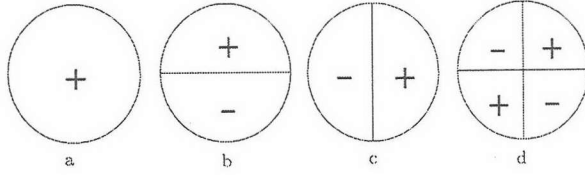


Fig. 6 The four orthogonal set of deformation modes. a) constant, b)  $\sin(\pi x/d)$ , c)  $\sin(\pi y/d)$  and d)  $\sin(\pi x/d)\sin(\pi y/d)$  ( $d$  is the diameter).

In this example, identification of boundary condition on the top face of a grooved cylinder and thereby the state of stress based on load incremental approach is demonstrated. Unless otherwise mentioned, a grooved cylinder (Fig. 4) made of plexiglas (photoelastic constant  $C_0 = 11$  [Brewster]<sup>1</sup>) is used for these set of numerical simulations. For this example this grooved cylinder is modelled with 11520 elements.

Starting from undeformed shape, deformation history in  $x$ ,  $y$  and  $z$  directions of the top face for four steps are assigned by superposing arbitrary proportions (amplitudes) of four orthogonal set of deforma-

<sup>1</sup> 1 [Brewster] =  $10^{-11}$  [m<sup>2</sup>/kg]

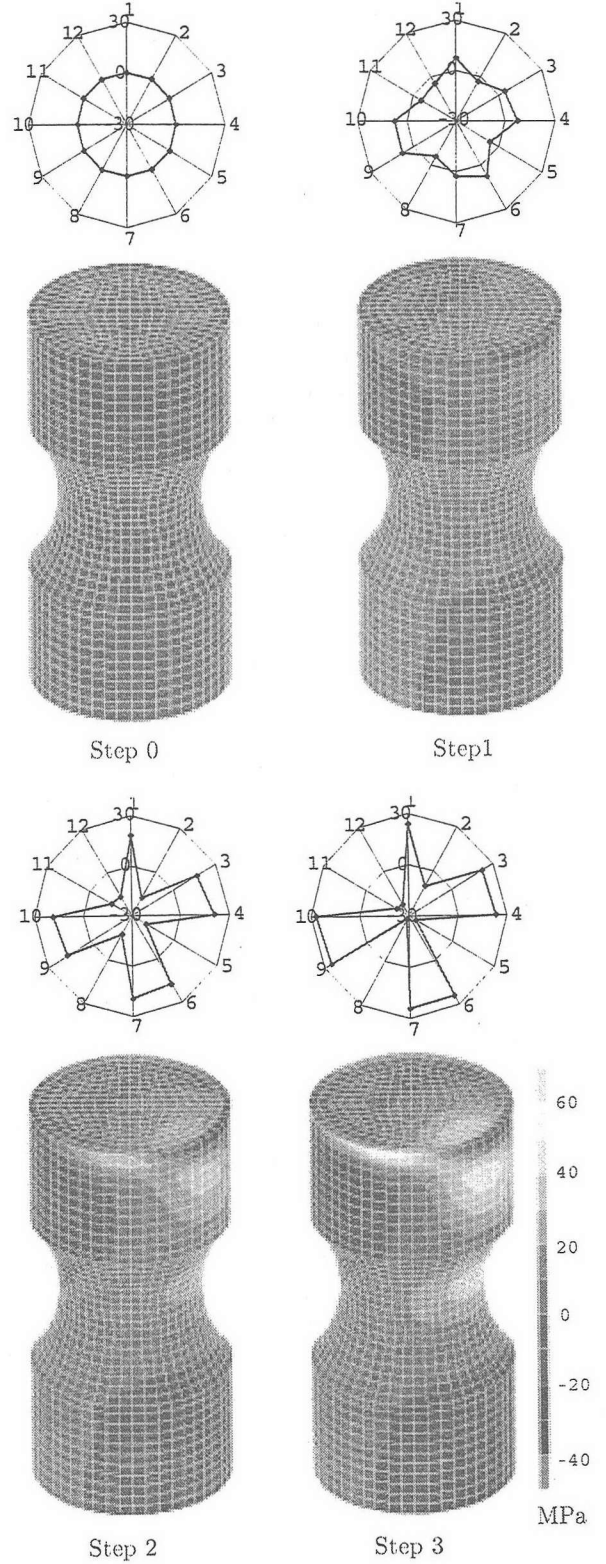
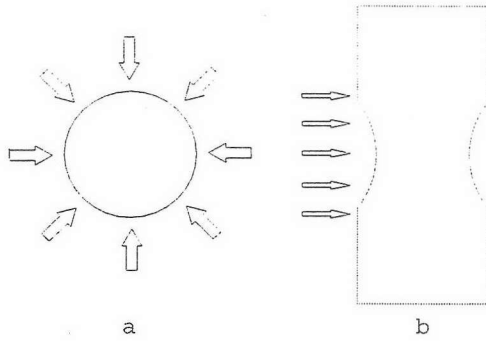


Fig. 7 History of  $\sigma_{33}$  and amplitudes of all the four modes in  $x$ ,  $y$  and  $z$  directions. Starting from 12 O' clock, radial axes in clockwise direction show amplitudes of modes 1, 2, 3 and 4 in  $x$ ,  $y$  and  $z$  directions.





**Fig. 8** Distribution of observations. a) Distribution of observation directions in the plan view. b) Distribution of light rays in front view. Rays passing through the grooved part are used in the inverse analysis.

tion modes, while the bottom face was assigned fixed boundary conditions. The four sets of orthogonal deformation modes used are shown in Fig. (6). Fig. (7) shows the history of  $\sigma_{33}$  and amplitudes of each mode.

The aim of the inverse analysis is to identify the increment in amplitude of each mode based on the new inversion method for identification of the history of boundary conditions, explained in the third section. Starting from the traction free condition, inverse analysis is incrementally performed using the transmitted light fringe patterns before and after each increment as input data set. Thus, history of the boundary conditions applied on the top face is reconstructed. The output light patterns are numerically calculated for each step in eight different observation directions perpendicular to the axis of the object(Fig. 8).

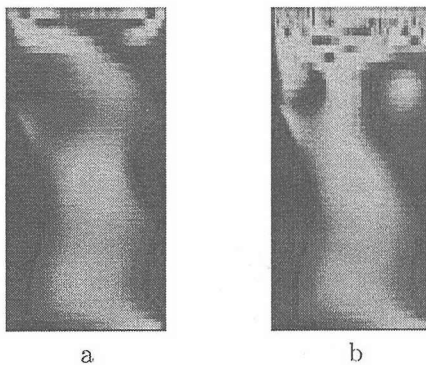


**Fig. 9** Fringe patterns generated by step 3 and the oscillating solution.

Exact convergence to each solution could be achieved during iterative calculations. The inverse

analysis performed between step0 and step3 without any intermediate steps showed an oscillatory behavior around a solution. Comparison of the fringe pattern corresponding to the exact state of stress at step 3 and the fringe pattern for one of the oscillating solution shows that the numerical scheme was oscillating around a different solution (Fig. 9). This is due to the inherent problem of  $2n\pi$  ambiguity in phase measurements. Ordinary approaches to 3D photoelasticity without using the history of state of stress or boundary conditions are not capable of identifying the state of stress when the relative phase difference is more than  $2\pi$ . Contrary to this, since the load incremental approach uses the history of state of stress or boundary conditions, arbitrary state of stress can be evaluated by selecting suitable load increments.

#### 4.2 Effect of noise in measurements

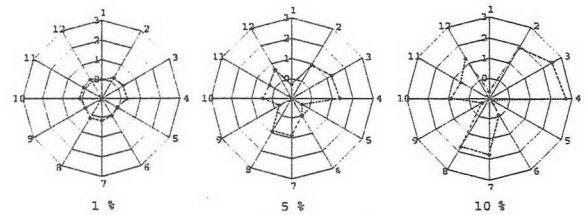


**Fig. 10** Percentage error in predicted results due to different amount of errors introduced to output light measurements. Starting from 12 O' clock, radial axes in clockwise direction show error in modes 1, 2, 3 and 4 in  $x$ ,  $y$  and  $z$  directions.

In order to understand the effect of presence of error in light intensity measurement, inverse analysis between step 1 and step 2 was performed with error introduced to all the output light measurements. Currently available 16 bit CCD cameras for scientific purposes has minimum of  $\pm 0.5\%$  error in light intensity measurements. On the other hand 8 bit CCD cameras for day to day usage has  $\pm 10 - 15\%$  error in light intensity measurements. Therefore, in this analysis three simulations with maximum error  $\pm 1\%$ ,  $\pm 5\%$  and  $\pm 10\%$  of the maximum light intensity were performed. Fig. 10 shows the maximum error in predicted modal weights for each case.

These results show that the error in predicted modal weights always remain less than the percentage error introduced to the output light measurements. On the other hand, error in output light measure-

ments are magnified by the load incremental approach for stress identification. The only difference between the method for stress identification and method for boundary condition identification is the use of equilibrium constraint in the latter method. Therefore, it is clear that the equilibrium constraint has a strong positive effect on stabilizing the numerical scheme in load incremental approach for identification of 3D state of stress.

### 4.3 Effect of limited observations

#### (1) Inverse analysis based on observation from a part of the body

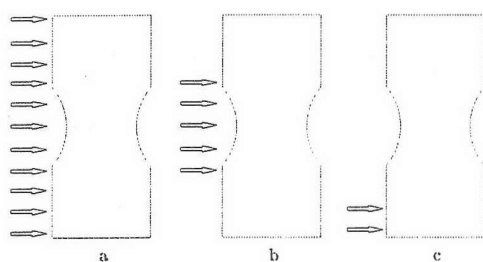


Fig. 11 Observations made at different regions of the grooved cylinder.

The new method discussed in this paper uses the superposition of state of stress due to independent set of boundary conditions. Therefore, theoretically, the boundary conditions must be able to be identified by scanning only a part of the body. This ability to identify the boundary conditions by scanning only a part of the body depends on the sensitivity of state of stress at that location to the modes of boundary conditions to be identified. To check the practical applicability of this method, inverse analysis between step 1 and 2 was performed using information on light transmitted by different parts of the grooved cylinder. The selected parts are (Fig 11); a) complete body, b) only the grooved part and c) 3mm thick disk at the fixed end. Observation from eight different directions uniformly distributed around the axis of the body shown in Fig. 8 were used.

The two cases with observations of grooved part (b) and the bottom most part (c) converged to the exact solution. This shows that the inverse analysis based on observations of remote portion of a body can identify the boundary conditions which can be modelled with lower modes (four lowest modes were used for this analysis). The use of this property has been demonstrated in the example problem by performing

the inverse analysis for 3 steps, only using light rays passing through the grooved part.

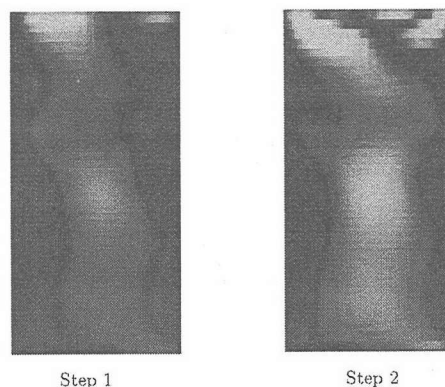


Fig. 12 Fringe patterns at step 1 and step 2.

Unexpectedly, the inverse analysis using complete body scanning failed to converged to the solution. Comparison of light patterns from step 1 and 2 (Fig. 12) shows that at the second step new dark bands has appeared on the top most region indicating that some light rays have undergone large phase increments. Such large phase increments always result in ambiguity in phase measurements which throws the numerical scheme away from the exact solution.

The convergence of two cases with observations made at remote locations from the top part shows that even when observations from some parts of the body cause ambiguity in phase measurements, the inverse analysis based on observations made at a different part of the body can successfully identify the boundary conditions.

#### (2) Inverse analysis based on limited number of observation directions

Since boundary conditions identification method uses the history of fringe patterns, observations have to be made while the specimen is mounted on the loading machine. Under such circumstances, it is difficult to have uniformly distributed set of observation directions all around the body. It would be very convenient in the experiment if the inverse analysis can be performed only using two or three observation directions. This will not only reduce the complexity of the experimental setup, but also the amount of computations (less number of light rays are used in the analysis) if faster convergence can be achieved. To identify the effect of reduction of number of observations, a numerical analysis with two observation directions perpendicular to each other was performed.

As in the example, only the light rays passing through the grooved part were used in the inverse analysis.

After 500 iterations the numerical scheme converged to the exact solution. This necessity of large number of iterations may be due to the existence of some modes which has a little effect on the fringe patterns in the selected two directions. If there were some modes which had almost no influence on the fringe patterns from these two directions, the numerical scheme could never have converged to the solution. Also, faster convergence could be achieved with large number of observations. Therefore, it is advisable to use a moderate number of observation directions that can be used in a less complicated experimental setup.

## 5. Conclusions and future work

A new nondestructive method for identifying boundary conditions applied on a linear elastic 3D body based on Photoelasticity is developed. This method uses the load incremental approach to linearize the nonlinear governing equation of photoelasticity by considering small load increments. In an earlier attempt, a method for stress identification in a 3D body was developed based on load incremental approach by the authors. In this new method, the earlier method is reinforced by applying the equilibrium constraint and identification of boundary conditions, thereby the state of stress is considered. As long as the load increments are small, this new method can be applied to identify the history of traction/displacement applied on a 3D body.

A direct application of this method is identification of boundary conditions on the surface of a crack in a

3D body under compression, thereby the state of stress around the crack. This identification of state of stress around a crack in a 3D body under compression will pave the way to explore the behavior of a crack in a 3D linear elastic body under compression.

To validate this new method and identify its limitations and behaviors which can be useful in the experiment, a set of numerical simulations were performed. Following conclusions could be arrived by these simulations.

1. The boundary conditions on a 3D elastic body can be identified using the history of fringe patterns from different directions.
2. Even when observations from some parts of the body cause ambiguity in phase measurements, the inversion based on observations made at a different part of the body can successfully identify the boundary conditions.

Less sensitivity to measurement errors and adequacy of less number of observations on a part of the body show the potential of this new method for practical applications. The next steps are experimental validation and application of this method to study crack propagation in bulk bodies under compression.

## REFERENCES

- 1) Aben H.: *Integrated Photoelasticity*, McGraw-Hill, New York 1979.
- 2) Wijerathne MLL, Kenji Oguni, Munee Hori.: Tensor field tomography based on 3D photoelasticity. *Mechanics of Materials*, Vol.34(9), pp.533-545, 2002

(Received April 18, 2003)